HBIs and sterols in surface sediments across the East Siberian Sea: implications for palaeo sea-ice reconstructions

Liang Su, Jian Ren, Marie-Alexandrine Sicre, Youcheng Bai, Bassem Jalali, Zhongqiao Li, Haiyan Jin, Anatolii S Astakhov, Xuefa Shi, Jianfang Chen

HBIs and sterols in surface sediments across the East Siberian Sea: implications for palaeo sea-ice reconstructions

Liang Su[1,2], Jian Ren[2*], Marie-Alexandrine Sicre[3], Youcheng Bai[2], Bassem Jalali[2,3], Zhongqiao Li[2], Haiyan Jin[2,6], Anatolii S. Astakhov[4], Xuefa Shi[5], Jianfang Chen[2,6*]

[1] Ocean College, Zhejiang University, Zhoushan 316021, China

[2] Key Laboratory of Marine Ecosystem Dynamics, Second Institute of Oceanography, Ministry of Natural Resources, Hangzhou 310012, China

[3] Sorbonne Université, Pierre et Marie Curie, CNRS, LOCEAN, Case 100, 4 place Jussieu, F-75005 Paris, France

[4] V.I. Il'ichev Pacific Oceanological Institute, Far Eastern Branch of Russian Academy of Sciences, 43 Baltiyskaya St., 690041 Vladivostok, Russia

[5] Key Laboratory of Marine Geology and Metallogeny, First Institute of Oceanography, Ministry of Natural Resources, Qingdao 266061, China

[6] State Key Laboratory of Satellite Ocean Environment Dynamics, Second Institute of Oceanography, Ministry of Natural Resources, Hangzhou 310012, China

Corresponding authors: Jian Ren (jian.ren@sio.org.cn);
Jianfang Chen (jfchen@sio.org.cn)

Key Points:

- Phytoplankton biomarkers indicate lower primary productivity in the East Siberian Sea than in the West-Chukchi Sea
- Continental run-off can bias PIP_{25} based sea-ice estimates in marginal seas
- Strongest correlation was found between $P_{III}IP_{25}$ and summer sea-ice at locations remote from river run-off influence

This article has been accepted for publication and undergone full peer review but has not been through the copyediting, typesetting, pagination and proofreading process, which may lead to differences between this version and the Version of Record. Please cite this article as doi: 10.1029/2021GC009940.

Abstract

Highly branched isoprenoids (HBIs) in marine sediments have emerged as promising semi-quantitative proxies to reconstruct seasonal sea-ice in polar oceans. In this work, we examine the distribution of sympagic HBIs (IP_{25} and HBI II), pelagic phytoplankton biomarkers (brassicasterol, dinosterol and HBI-III) as well as terrestrial sterols (campesterol and β-sitosterol) in the surface sediments of the East Siberian Sea (ESS) to test their reliability as sea-ice proxies under continental run-off influence. Our data suggest that dinosterol performs better than brassicasterol to assess sea-ice across the ESS shelf, yet the correlation between P_DIP_{25} and spring sea-ice is relatively weak but improves when removing sites with salinity <25. Strongest relationship is found between $P_{III}IP_{25}$ and summer sea-ice in regions remote from riverine influence. Overall, our results show that semi-quantitative estimates of sea-ice based on biomarkers can be problematic in Arctic Ocean margins because of biases induced by continental run-off on biological productivity and sea-ice production.

Plain Language Summary

Biomarkers in sediments provide information on past surface water environmental and biological conditions. They show that primary production in the West-Chukchi Sea is higher than in the East Siberian Sea due to sea-ice retreat as a result of global warming and nutrient-rich Pacific water inflow. They also emphasize that sea-ice estimates in continental shelf sediments can be biased by continental run-off.

Key words: Sea-ice, biomarkers, IP_{25}, PIP_{25} index, East Siberian Sea, Arctic Estuary

1. Introduction

Since the beginning of the 20th century, the global ocean has undergone unprecedented changes caused by global warming (Gillett et al., 2021; Stocker et al., 2013). These changes are notably pronounced in the Arctic region due to polar amplification with major consequences for sea-ice cover and the thermohaline circulation (Cavalieri et al., 1997; Shindell & Faluvegi, 2009). The Arctic Ocean and its marginal seas are characterized by large seasonal sea-ice changes. Melting in summer and sea-ice formation in winter, including coastal polynyas, through the production of cold and saline waters, alter deep-water formation and subsequently the Arctic Ocean circulation (Arrigo, 2014; Cai et al., 2010; Overland & Wang, 2013; Xiao et al., 2013). At the current rate of decline (0.42% $year^{-1}$), the Arctic Ocean may be ice-free in summer season in the next 50 or even 30 years (Comiso, 2012; Wang et al., 2019), which will profoundly impact the global climate and carbon cycle and further accelerate global warming causing damages to the polar ecosystems (Moline et al., 2008). In Arctic marginal seas changes in sea-ice cover and thickness involve different thermodynamic and dynamic factors (Polyakov et al., 2003). In the case of the East Siberian Sea (ESS), land run-off and atmospheric circulation are controlling factors of the sea-ice distribution (Park et al., 2020; Rigor & Wallace, 2004).

Our knowledge on natural variability of Arctic sea-ice and on-going changes are limited by the lack of long time series. Information on past sea-ice distribution can be obtained from micropaleontological fossils (Cronin et al., 2013; de Vernal et al., 2020; Nair et al., 2019), geochemical indexes (Hillaire-Marcel & de Vernal, 2008) or biomarker proxies such as IP_{25} (Ice Proxy with 25 carbon atoms), a mono-unsaturated highly-branched isoprenoid (HBI) produced by sea-ice diatoms (Belt et al., 2007). Although known modern producers of IP_{25} only account for ~3.6% of the total diatoms living in the Arctic (Brown et al., 2014), a significant positive correlation between sea ice diatoms and sympagic IP_{25} has been found in the sediment trap data from the western Arctic Ocean (Fahl & Nöthig, 2007; Ren et al., 2020; Zernova et al., 2000). Since the first IP_{25}-based sea-ice reconstruction of Massé et al. (2008) off North Iceland, the PIP_{25} (Phytoplankton-IP_{25}) index combining IP_{25} with phytoplankton markers (brassicasterol or dinosterol) has been proposed to derive semi-quantitative estimates of sea-ice (Müller et al., 2011). More recently, the substitution of sterols by the tri-unsaturated HBI alkene (HBI-III) in the PIP_{25} index has been proposed to better reflect ice-free pelagic phytoplankton than sterols (Bai et al., 2019; Koch et al., 2020; Smik et

al., 2016a). Numerous studies have been carried out to produce past sea-ice reconstructions (for reviews and further references see Stein et al., 2012; Belt and Müller, 2013; Belt, 2018) including in the Arctic Ocean (Belt and Müller, 2013; Belt, 2018; Stein et al., 2016, 2017; Xiao et al., 2015a). The applicability of HBIs and sterols in the pan-Arctic surface sediments for assessing (paleo) sea-ice has also been discussed (Xiao et al., 2015b; Kolling et al., 2020; Stoynova et al. 2013). Yet, the production, export and preservation of HBIs are still poorly documented and require further investigations to achieve robust sea-ice reconstructions. In this regard, although the influence of continental run-off on the HBIs and phytosterol production and its impact on PIP_{25} values has been initially discussed in Xiao et al. (2013) and Hörner et al. (2016), uncertainties remain due to the lack of observations. This study presents a mapping of HBIs and sterol concentrations in 42 surface sediments from the ESS and adjacent West-Chukchi Sea (thereafter West-CS; see Fig. 1) and assess existing proxies of seasonal sea-ice under high continental run-off.

2. Regional settings

The ESS is one of the heaviest sea-ice covered marginal seas of the Eurasian continent. It is largely influenced by both Eurasian rivers run-off and the Arctic Oscillation (AO) which in turn modulate the ocean circulation over most of the basin (Dukhovskoy et al., 2006; Thompson & Wallace, 1998). The water circulation in the ESS consists of the Siberian Coastal Current (SCC) that runs alongshore from west to east, the Pacific Water Inflow (PWI) through the Bering Strait (BS) and the discharge of two large rivers, the Indigirka River (IR) and the Kolyma River (KR) (Münchow et al., 1999) (Fig. 1). Originated from the Laptev Sea (LS) through the Dmitry Laptev Strait, the SCC flows eastwards into the ESS and mixes on its path with Siberian river freshwaters and sea-ice melt waters. Forced by winds, the SCC continues and crosses Long Strait before dissipating in the CS (Weingartner et al., 1999). When entering the Arctic Ocean, the PWI splits into three branches: the western branch Anadyr Water (AW, high salinity and high-nutrient), the middle branch Bering Shelf Water (BSW, medium salinity), and the eastern branch Alaskan Coastal Water (ACW, low salinity and low-nutrient) (Coachman & Aagaard, 1966; Grebmeier et al., 2006; Woodgate et al., 2005) (Fig. 1).

AO is a key feature of the Arctic region climate. High AO favors a cyclonic circulation in the Russian Arctic diverting eastward the freshwater delivered by Eurasian rivers off the shelf (Morison et al., 2012). The IR and the KR, with an annual

run-off of 61 km^3 $year^{-1}$ and 132 km^3 $year^{-1}$, respectively (Gordeev et al., 1996), are important sources of terrigenous material into the ESS (Bröder et al., 2019). To the west, the Lena River (LR), with a water discharge of 588 km^3 $year^{-1}$ represents the largest fresh water volume to the LS and the ESS (Holmes et al., 2011). These freshwater inputs affect processes such as freezing, sea-ice formation, melting and transport of sea-ice (Aagaard & Carmack, 1989) and thus the distribution of coastal sea-ice (Divine et al., 2004; Haine et al., 2015).

Sea-ice in the ESS exhibits strong seasonal and interannual variability (Parkinson et al., 1999; Wang et al., 2019). The ESS is entirely frozen from November to April. In May, sea-ice around the northern New Siberian Islands begins melting under the influence of winds. In June, inshore sea-ice starts thawing and declining. Open water conditions generally establish earlier in the West than in the East-ESS. Sea-ice begins freezing in October at a higher freezing rate in the West-ESS. Summer sea-ice coverage in the Arctic Ocean has been decreasing significantly in the past decades leading to ESS evolving from a largely ice-covered area to an area now largely ice-free (Wang et al., 2018).

Sea-ice motion in ESS is affected by wind patterns generally following the wind direction (Morris et al., 1999). On the shallow Siberian continental shelf, the persistent sea breeze in winter causes the formation of polynya or channels at the boundary between land-fast ice and pack ice (Zhang et al., 2021) such as the Great Siberian Polynya that has long existed between the eastern LS and the New Siberian Islands (Bareiss & Görgen, 2005; Zonn et al., 2016; Speer et al., 2017). **3. Material and methods**

3.1 Sediment sampling

A total of 42 surface sediment samples (0-2 cm) were retrieved from the ESS during the Cruise LV77 aboard the R/V *Akademik M.A. Lavrentiev* (Fig. 1). The samples were collected using a box-corer and quickly stored at -20 °C after recovery. They were freeze-dried prior biomarker analyses in the Key Laboratory of Marine Ecosystem Dynamics, Second Institute of Oceanography, Ministry of Natural Resources (Hangzhou, China).

3.2 Total organic carbon (TOC) and Total nitrogen (TN) analyses

The TOC and TN were analyzed at the Ocean College, Zhejiang University. For these bulk analyses, samples were also freeze-dried and homogenized. Approximately 1 g of sediment was acidified with 1 mol L^{-1} HCl and left at 50 °C for at least 48 hours

to remove carbonates. Samples were then washed with ultra-pure water to pH = 7 and then freeze-dried (Williford et al., 2007). Samples were analyzed with an element analyzer (FLASH 2000 CHNS-O, Thermo Fisher) for TOC and TN determination. Reference samples BBOT Thermo were used for quality control. The standard deviation of the measurements is less than < 0.1%.

3.3 Biomarker analyses

Lipids were extracted from the freeze-dried sediments using a mixture of dichloromethane/methanol (2:1 v/v) for 10 min in an ultrasonic bath, then centrifuged for 2 min at 2500 rpm. The supernatant containing the lipids was then retrieved with a clean glass pipette and placed in a clean glass vial. This step was repeated twice, the three extracts were combined and dried under a gentle nitrogen stream. Hydrocarbons, alkenones and sterols were further separated from the total lipid extract using 2.5 ml n-hexane, 4 ml n-hexane/ethyl acetate (90:10 v/v) and 4 ml n-hexane/ethyl acetate (70:30 v/v), respectively, using silica gel as stationary phase (Sicre et al., 2001). After separation, 50 µl BSTFA (bis-trimethylsilyl-trifluoroacetamide) were added to the sterol fraction and heated at 70 °C for 1 hour to complete derivatization. Both C_{25}-HBIs (IP_{25}, HBI-II, HBI-III and HBI-IV, a geometric isomer of HBI-III) and sterols were analyzed by gas chromatography (GC, Agilent Technologies 7890) coupled to mass spectrometry (MS, Agilent 262 Technologies 5975C inert XL) (Belt et al., 2007; Müller et al., 2011). GC/MS analyses were carried out on a 30 m HP-5MS column (0.25 mm i.d., 0.25 µm film thickness). The oven temperature was programmed from 40 °C to 300 °C at a heating rate of 10 °C min^{-1} and maintained at final temperature for 10 min. The operating conditions of MS were as follows: ion source temperature at 250 °C and ionization energy at 70 eV. Individual compounds were identified based on their retention time with reference compounds and their mass spectra. For quantification of HBIs (*m/z* 350 for IP_{25}, *m/z* 348 for HBI-II, and *m/z* 346 for HBI-III and HBI-IV), 7-hexylnonadecane (*m/z* 266) was used as an internal standard and added to the sample prior extraction while cholesterol-d6 (cholest-5-en-3β-ol-D6, *m/z* 464) was used as an external standard and added prior injection to calculate sterol concentrations. The molecular ions *m/z* 470, *m/z* 500, *m/z* 396, and *m/z* 382 were used to quantify the sterols, brassicasterol (24-methylcholesta-5,22E-dien-3β-ol), dinosterol (4α,23,24R-trimethyl-5α-cholest-22E-en-3β-ol), 24-ethylcholest-5-en-3-ol and campesterol (24-methylcholest-5-en-3β-ol), respectively. It should be noted that both the α and β isomers of the 24-ethylcholest-5-en-3-ol co-exist in marine sediments. However, the β

isomer (24-ethylcholest-5-en-3β-ol) named β-sitosterol of terrigenous origin is found in high abundances in coastal settings except for coastal upwelling areas where the α isomer can prevail due to high productivity (Volkman, 1986). Diatoms can produce β-sitosterol, though in minor amounts, as opposed to cyanobacteria as reported in cyanobacterial mats (Boon et al., 1983). We assume that 24-ethylcholest-5-en-3-ol is primarity β-sitosterol in our samples (see discussion). All concentrations of biomarkers were then normalized to TOC.

3.4 Calculation of the PIP_{25} index

Semi-quantitative estimates of sea-ice were calculated using the PIP_{25} index that combines sympagic IP_{25} and pelagic phytoplankton biomarker (P) in the following expression (Müller et al., 2011):

$$PIP_{25} = \frac{[IP_{25}]}{[IP_{25}] + [phytoplankton\ biomarker] * c}$$

$$where\ c = \frac{mean\ IP_{25}\ concentration}{mean\ phytoplankton\ biomarker\ concentration}$$

Brassicasterol, dinosterol and HBI-III were used as a reference for pelagic phytoplankton to derive P_BIP_{25}, P_DIP_{25} and $P_{III}IP_{25}$ indexes, respectively. The *c* value represents the ratio of the mean concentration of IP_{25} over the mean concentration of the selected phytoplankton biomarker of all samples, or the subset after ruling out estuarine samples (salinity <25). Since the abundances of IP_{25} and HBI-III were of similar magnitude in our data set, the $P_{III}IP_{25}$ index was also calculated for c =1.

3.5 Oceanographic data

The satellite sea-ice concentration (SIC) data were obtained from the Nimbus-7 SMMR and DMSP SSM/I-SSMIS passive microwave data of the National Snow and Ice Data Center (NSIDC, https://nsidc.org). Here, we selected the average SIC from 1996 to 2015 to generate SIC for spring (Sp; April, May and June) and summer (Su; July, August and September) and the 20% isolines of September SIC shown in Figure 1.

Based on the range of sedimentation rate in most of the study area (1.1 to 1.6 mm $year^{-1}$; Bröder et al., 2016; Vonk et al., 2012), the top 2 cm of the surface sediments represent between ~20 and ~30 years. During this period, the Arctic sea-ice experienced relatively stable icy years in 1990-1999 followed by a decade of significant sea-ice retreat in 2007-2016 (NSIDC, https://nsidc.org). These two situations are shown in Figure 1 by the average summer minimum sea-ice (20% of SIC) from 1990 to 1999 and

from 2007 to 2016, respectively.

The chlorophyll *a* data were obtained from the Moderate Resolution Imaging Spectroradiometer (MODIS) on the Aqua satellite, using the GlobColour processing results (https://hermes.acri.fr/). The May to September mean value of chlorophyll *a* from 1998 to 2016 was used. Summer sea surface salinity (SuSSS) and temperature (SuSST) data are from World Ocean Atlas 2013 (WOA13, https://www.nodc.noaa.gov/OC5/woa13/) with 0.25° grid. A map showing the different regions and their acronyms used in the discussion is provided in Fig. S1.

4. Results

4.1 Total organic carbon (TOC) and total nitrogen (TN)

The values of TOC and TN in the ESS span from 0.2 to 2.1% and from 0.03 to 0.22%, respectively (Fig. 2a and 2b; Table S1). Maximum TOC values of 1.7 to 2.1% are found in the East-ESS/West-CS, while lowest ones (< 0.5%) occur off the KR mouth and highest latitudes. The spatial distribution of TN values shares strong resemblance with TOC (Table S1).

4.2 Sterols

Brassicasterol shows high values in the central ESS (141-191 μg g^{-1} TOC, Table S1, Fig. 3a), while dinosterol is generally low across the basin except for high values east of Wrangel Island under the influence of AW (9-14 μg g^{-1} TOC; Table S1, Fig. 3b). Terrestrial campesterol and β-sitosterol both show extremely low values in the northernmost area as for brassicasterol and dinosterol. However, campesterol and β-sitosterol strongly differ along the shelf suggesting different sources (Fig. 3c, d).

4.3 C_{25} highly branched isoprenoid (HBI) alkenes

The distribution patterns of sympagic IP_{25} and HBI-II are generally similar, with high values in the central ESS and near the New Siberian Islands (IP_{25}: 1.7-2.4 μg g^{-1} TOC; HBI-II: 1.7-2.7 μg g^{-1} TOC, Table S1 and Fig. 4a, b). Values decrease from the central region to nearshore sediments (IP_{25}: 0.2-0.7 μg g^{-1} TOC; HBI-II: 0.1-0.4 μg g^{-1} TOC, Table S1) and reach a minimum at high latitudes (IP_{25}: 0.06-0.4 μg g^{-1} TOC; HBI-II: 0.08-0.5 μg g^{-1} TOC, Table S1). IP_{25} and HBI-II are also low in the West-CS.

HBI-III and HBI-IV show very similar patterns with a maximum south and east of Wrangel Island that strikingly contrast with the sympagic HBIs (0.11-1.68 μg g^{-1} TOC; Fig. 4a, b). Intermediate values occur in the central ESS (1.8-2.7 μg g^{-1} TOC) while lowest ones are found in coastal waters and at highest latitudes (Fig. 4c, d). The HBI-IV sediment content is generally <2 μg g^{-1} TOC (Fig. 4c, d, Table S1) except for south

and east Wrangel Island (Fig. 4c, d, 6.8-8.5 μg g^{-1} TOC, Table S1), as also found for HBI-III.

5. Discussion

5.1 Organic carbon sources

TOC in the ESS coastal surface sediments results from mixed inputs of marine primary production and terrigenous sources (Vonk et al., 2012). *n*-Alkanes in sediments indicate a gradually decrease of terrestrial organic carbon from south to north, along a transect from the IR estuary to offshore (Petrova et al., 2004). Similar trends are observed in the C/N ratios (Fig. 2c) and terrestrial sterols (Fig. 3). In the outer East-ESS and West Wrangle Island, the prevailing source of TOC is generally marine as indicated by C/N ratio <8 (Fig. 2c), high dinosterol (>5 μg g^{-1} TOC, Fig. 3b) and brassicasterol concentrations (>100 μg g^{-1} TOC, Fig. 3a). This result is consistent with warm and nutrient-rich PWI flowing into the CS through the Bering Strait sustaining high primary production and export in the East-ESS and West-CS, leading to organic rich sediments till around 170 °E (Fig. 2a) (Bröder et al., 2019; Sparkes et al., 2016; Stein and Macdonald, 2004; Tesi et al., 2014).

In the nearshore West-ESS sediments, high C/N ratio >10 and β-sitosterol concentrations (>200 μg g^{-1} TOC) highlight strong imprint of terrigenous material (Fig. 3d and 2c). Marginal seas such as the Kara and Laptev Seas are also strongly affected by land run-off and nearshore area (Fernandes and Sicre, 2000; Peulvé et al., 1996) as indicated by high C/N ratio and *n*-alkanes (C_{27} + C_{29} + C_{31}) (Stein & Fahl, 2004a, 2004b). This is also in agreement with previous reports of lower $\delta^{13}C$ of TOC values (-27.4‰ ~ -25.5‰; Bröder et al., 2019) and high lignin concentrations (0.9-1.2 mg g^{-1} TOC; Salvadó et al., 2016) in the ESS.

In areas of significant amount of seasonal sea-ice (73-76°N), high TOC is generally associated with enhanced primary production as reflected by concomitant high TN. At highest latitudes, North of 77°N, the low TOC sediment content reflects minor terrigenous organic carbon and limited primary production and export due to permanent sea-ice. The distribution of spring and summer chlorophyll *a* in surface waters suggest enhanced primary production in the coastal waters of the ESS (Fig. 2d). However, higher brassicasterol levels are found in the central ESS rather than in the coastal areas reflecting enhanced marine production in the marginal ice zone (MIZ) (Fig. 3a). This mismatch between phytosterol and chlorophyll patterns can in part be

explained by the known bias of optically-complex (Case 2) waters induced by high suspended particle load of more turbid coastal waters leading to the overestimation of chlorophyll *a* concentrations. Terrestrial colored dissolved organic matter (CDOM) is another source of bias of chlorophyll *a* concentrations caused by the abnormally high absorption of CDOM at low phytoplankton biomass such as in shelf waters (Lewis & Arrigo, 2020). Overall, primary production in the ESS is strongly affected by terrigenous suspended particles delivered in nearshore waters. Highly turbid waters together with fluctuating salinity likely explain brassicasterol minima off the IR and KR river mouths, a result that can introduce complication in the interpretation of sea-ice proxy indexes using sterols.

5.2 Phytoplankton biomarkers

Brassicasterol is primarily produced by marine diatoms thriving in open sea waters or at the sea-ice edge, while dinosterol is commonly synthesized by dinoflagellates in open sea waters (Volkman, 1986). In contrast to the Kara and Laptev Seas (Xiao et al., 2013), these two phytosterols do not show similar distributions in the ESS (Fig. 3a, b). No clear correlation between IP_{25} and brassicasterol was found by Xiao et al. (2015b) and Kolling et al. (2020). In addition, in our study the distribution pattern of brassicasterol seems to match with that of IP_{25} and HBI-II while dinosterol shares stronger resemblance with HBI-III and HBI-IV (Fig. 2a, 2b, 3). These findings agree with brassicasterol production being associated with nutrient-rich conditions of the sea-ice edge while turbid waters off the IR and KR deltas do not provide favorable conditions to marine diatom growth. Therefore, different local and regional phytoplankton source and distribution are expected from different drainage basin, water discharge and suspended load of Eurasian rivers (Xiao et al., 2015b; Kolling et al., 2020). Although dinosterol is also affected by estuarine conditions, its concentration remain relatively homogeneous across the ESS. It is noteworthy that this sterol in our samples is an order of magnitude lower than found by Stoynova et al. (2013) by using different extraction methods and internal standard quantification.

HBI-III is produced by diatoms living at the sea-ice edge and in ice-free waters (Bai et al., 2019; Belt, 2018; Smik et al., 2016a). A one-year sediment trap time series from the CS has consistently shown higher production of HBI-III at low sea-ice concentrations (Bai et al., 2019). This finding is in line with low to moderate values of HBI-III (and HBI-IV) in the central to East-ESS, between the two isolines of September minimum ice edge (Fig. 4c) and previous interpretation of HBI-III distribution (Arrigo

et al., 2014; Collins et al., 2013; Smik et al., 2016b). Highest HBI-III and HBI-IV are likely reflecting the earlier retreat of sea-ice in the West-CS than in the ESS and the inflow of nutrient-rich PWI providing favorable conditions for their production. By contrast, HBI-III and HBI-IV concentrations are extremely low in nearshore and coastal waters as opposed to sympagic HBIs that show moderate levels. Only in the permanent sea-ice area, do all HBIs show low levels. In summary, HBI-III and HBI-IV as well as dinosterol were low or absent in the permanent sea-ice and nearshore waters while enhanced in West-CS. Intermediate values were found in the MIZ where brassicasterol and sympagic HBIs were abundant in accordance with our present knowledge on these biomarkers. HBI-III production is thus consistent with open water conditions (Belt, 2018; 2019; Köseoğlu et al., 2018; Smik et al., 2016a) although recently Amiraux et al. (2021) reported the occurrence of this HBI in sea-ice in southwest Baffin Bay.

5.3 IP_{25} variability and spring/summer sea-ice condition

IP_{25} is found throughout the ESS (Fig. 4a). The distribution patterns of IP_{25} and HBI-II are generally similar (Belt et al., 2016) as reported in earlier studies in the Arctic Ocean (Xiao et al., 2015b; Koch et al., 2020) as opposed to Baffin Bay (Kolling et al., 2020). At high latitudes (North of 77°N), lowest IP_{25} together with lowest phytosterols and other HBIs are consistent with permanent sea-ice. In the outer continental shelf, melting does not take place until the end of summer resulting in an extremely short phytoplankton growing season. In the eastern New Siberian Islands maximum IP_{25} can be explained by favorable production conditions. Indeed, longest season of fast ice formation has been observed between the New Siberian Islands and the coast (Yu et al., 2014). In addition, wind-driven polynya formation and channels between land-fast ice and pack ice also cause sea-ice diatom blooms (Zhang et al., 2021).

In the central ESS, simultaneous high concentrations of IP_{25}, HBI-II and brassicasterol and moderate HBI-III concentrations underpin MIZ conditions (Fig. 3a, 4a-c). Similarly, maximum abundance of IP_{25} during summer is consistent with sediment trap data under MIZ conditions characterized by sea-ice algae production throughout the Arctic Ocean (Bai et al., 2019; Fahl & Stein, 2012; Koch et al., 2020; Nöthig et al., 2020). We can thus conclude that seasonal sea-ice edge and/or MIZ conditions prevailed in the central ESS over the last decades.

Lower IP_{25} values in the nearshore are expected from North-South sea-ice cover trends across the ESS in spring/summer. Xiao et al. (2015b) also found low IP_{25} production in the LS due to freshening by riverine waters. Other factors such as water

turbidity in the river plume, erosion and sediment resuspension in shallow waters caused by upwelling along the coast all concur to reduce phytoplankton production (Osadchiev et al., 2020a, b). Lowest sympagic HBIs in West-CS are coherent with the early sea-ice retreat caused by summer SSTs reflecting the influence of the PWI. In general, we found a very weak correlation between IP_{25} and spring or summer SIC (SpSIC: r^2=0.09, p<0.01; SuSIC: r^2<0.01, p<0.01; Table 1).

5.4 PIP_{25} indexes

At latitudes North of 77°N, all PIP_{25} values were > 0.75 (Fig. 5a, b, c; Fig. S2) reflecting permanent sea-ice cover. IP_{25} and phytoplankton biomarkers show intermediate to high concentration values in areas lying between the summer 20% SIC isoline of 1990 - 1999 (time interval of stable icy conditions) and that of 2007 - 2016 (time interval when sea-ice extent decreased rapidly) (Fig. 3, 4). In this area, PIP_{25} values are comprised between 0.4 and 0.7 reflecting the gradual northward retreat of sea-ice providing optimum living conditions for sea-ice diatoms and phytoplankton growth in agreement with previous observations in the CS (Hill et al., 2018).

$P_{III}IP_{25}$ and P_DIP_{25} in the West-CS depict broadly similar distribution with values <0.2 indicating low sea-ice to open water conditions and high phytoplankton production. At nearshore sites of the ESS, owing to the influence of fresh water and terrigenous inputs from the IR and KR, the production and export of biomarkers differ from those of open ocean waters. Surface salinity is another factor that may affect phytoplankton distribution as shown in Figure 6 by the abundances of IP_{25}, HBI-III, brassicasterol and dinosterol along the 166°E meridian (from Zweng et al., 2013) and thus bias PIP_{25}. For instance, low or undetectable HBI-III led to abnormally high $P_{III}IP_{25}$ values (Fig. 4c; Fig. 5c) that are close to those of permanent sea-ice (Fig. 5d). This result underscores unfavorable conditions for pelagic phytoplankton to prosper such as stratification and enhanced turbidity of Eurasian rivers plumes spreading and mixing with the narrow SCC over the shelf. Biases are also evident from intermediate values of P_BIP_{25} off the IR mouth resulting in misleading estimates of high seasonal SIC. However, dinosterol remains rather high over the shelf suggesting possible adaptation of dinosterol producers (dinoflagellates) to variable salinity and suspended load (Kraberg et al., 2013; Nelson & Sachs, 2014; Wu et al., 2020). Interestingly, P_DIP_{25} values are low at sites influenced by IR and KR run-off except for one site near the IR mouth (Fig. 5b). In the LR estuary, however, the concentrations of dinosterol remain low compared to those of brassicasterol possibly reflecting freshwater producers of the

latter (Fig. S3; Xiao et al., 2015b). Such departures should be carefully considered when using PIP_{25} index to reconstruct paleo-sea-ice in deltaic settings (Belt, 2018; Xiao et al., 2015b; Kolling et al., 2020).

Weak correlations were found between PIP_{25} and SIC (either SpSIC or SuSIC, r^2<0.41, p<0.01), except for P_DIP_{25} (Tables 1, S2; n= 42, r^2=0.51, p<0.01). However, our set of surface sediments encompasses a range of deposition rates. In addition, from coastal waters to open sea, the ESS covers variable environmental and sea-ice conditions (Petrova et al., 2004; Stein, 2008). The deposition rate over the continental shelf is about 1.1 to 1.6 mm $year^{-1}$ (Bröder et al., 2016; Vonk et al., 2012) and decreases to 0.09-0.02 mm $year^{-1}$ towards the deep-sea basin (Li et al., 2020; Stein & Fahl, 2000). Owing to different deposition rates within our sites, the top 2 cm of sediment may represent different time interval, which can account in part for the departure from linear relationship between PIP_{25} and SIC. Of course, the source uncertainty of brassicasterol in coastal waters also reduced the correlation between P_BIP_{25} and SuSIC (Volkman, 1986). The relationship is improved after removal of sites with salinity less than 25 (summer salinity gradient between the estuary and open ocean, from World Ocean Atlas 2013 by Zweng et al., 2013) (Tables 1, S3 and Fig. S3). Overall, our findings suggest that P_DIP_{25} might be more suitable for sea-ice reconstruction in coastal waters influenced by river run-off (Table 1). High concentrations of terrestrial sterols (campesterol and β-sitosterol) have been found in the Siberian marginal sea estuaries (Fig. 3c and 3d; Xiao et al., 2013, 2015b), implying them as proxies for riverine input. Therefore, terrestrial sterols (or other terrestrial proxies) should be considered when using IP_{25}/PIP_{25} to reconstruct paleo-sea-ice environment to discern the influence of continental run-off.

6. Conclusions

Spatial mapping of sympagic HBIs and pelagic phytoplankton biomarkers from 42 surface sediments revealed differences across the ESS and the West-CS. High productivity was inferred from dinosterol, HBI-III and HBI-IV concentrations in West-CS sediments as a result of the nutrient-rich PWI and early retreat of sea-ice allowing for a longer algal production season. Low marine production characterized nearshore sites of the ESS most likely due to Eurasian River plumes and their eastward propagation along with the SCC. Stratification induced by freshwater from the IR and KR rivers combined with high suspended load likely account for reduced primary

production in the ESS shelf waters.

Highest concentrations of IP_{25}, brassicasterol, dinosterol and HBI-III found around 74°N, coincide with the average summer ice edge (20% SIC isoline) for the 2007 to 2016 interval, reflecting the average MIZ conditions. IP_{25} and PIP_{25} indexes in the ESS did not show significant correlations with SpSIC or SuSIC except for P_DIP_{25}. This result suggests that dinosterol production was less affected by riverine inputs. Noteworthy, the generally low values of phytoplankton biomarkers in nearshore sediments at comparable levels as those found in permanent sea-ice areas at high latitudes underscore the potential PIP_{25} biases and subsequently erroneous SIC estimates. Our study overall warns cautiously about the use of PIP_{25} in regions where continental run-off is significant.

Acknowledgements

We acknowledge the crew and the Russian-Chinese scientific party of R/V *Akademik M.A. Lavrentiev* for their professional sampling work. We are indebted to Jiaqi Wu of Second Institute of Oceanography for her helpful advice and to Prof. Hao Zheng and Yiwen Pan of Zhejiang University for their kind help in the TOC measurement. Vincent Klein of Sorbonne Université is also thanked for technical assistance. This study is financially supported by the National Natural Science Foundation of China (Nos. 41606052, 41941013, 41976229, 42076242), the National Key Research and Development Program of China (No. 2019YFC1509101), the Marine S&T Fund of Shandong Province for Pilot National Laboratory for Marine Science and Technology (Qingdao) (No. 2018SDKJ0104-3), the Scientific Research Funds of the Second Institute of Oceanography, State Oceanic Administration, China (Nos. JG1611, JG1911, JG1806) and the Russian Science Foundation (Grant 21-17-00081). MAS thanks the Centre National de la Recherche Scientifique (CNRS) for salary support. We are grateful to Rüdiger Stein and two anonymous reviewers who provided useful suggestions for the manuscript improvement.

Data availability statement

All data in this study are presented in supporting information files and are available under https://doi.org/10.1594/PANGAEA.934576.

Author contributions

L.S., J.R. and J.C. designed the study and wrote the manuscript with contribution of M.-A.S., Y.B., B.J., Z.L., H.J., A.A.S. and X.S. L.S. contributed the biomarker analyses and the determination of TOC. J.R. retrieved the environmental data from different database. All authors contributed to the final version of the manuscript.

Declarations of interest: None

References

Aagaard, K. & Carmack, E. C. (1989), The role of sea ice and other fresh water in the Arctic circulation, *Journal of Geophysical Research: Oceans*, *94*(C10), 14485-14498. doi: 10.1029/JC094iC10p14485.

Amiraux, R., Archambault, P., Moriceau, B., Lemire, M., Babin, M., Memery, L., et al. (2021), Efficiency of sympagic-benthic coupling revealed by analyses of n-3 fatty acids, IP_{25} and other highly branched isoprenoids in two filter-feeding Arctic benthic molluscs: *Mya truncata* and *Serripes groenlandicus*, *Organic Geochemistry*, *151*, 104160. doi: 10.1016/j.orggeochem.2020.104160.

Arrigo, K. R. (2014), Sea ice ecosystems, *Annual review of marine science*, *6*, 439-467. doi: 10.1146/annurev-marine-010213-135103.

Arrigo, K. R., Perovich, D. K., Pickart, R. S., Brown, Z. W., van Dijken, G. L., Lowry, K. E., et al. (2014), Phytoplankton blooms beneath the sea ice in the Chukchi sea, *Deep Sea Research Part II: Topical Studies in Oceanography*, *105*, 1-16. doi: 10.1016/j.dsr2.2014.03.018.

Bai, Y., Sicre, M.-A., Chen, J., Klein, V., Jin, H., Ren, J., et al. (2019), Seasonal and spatial variability of sea ice and phytoplankton biomarker flux in the Chukchi sea (western Arctic Ocean), *Progress in Oceanography*, *171*, 22-37. doi: 10.1016/j.pocean.2018.12.002.

Bareiss, J. & Görgen, K. (2005), Spatial and temporal variability of sea ice in the Laptev Sea: Analyses and review of satellite passive-microwave data and model results, 1979 to 2002, *Global and Planetary Change*, *48*(1-3), 28-54. doi: 10.1016/j.gloplacha.2004.12.004.

Belt, S. T. (2018), Source-specific biomarkers as proxies for Arctic and Antarctic sea ice, *Organic Geochemistry*, *125*, 277-298. doi: 10.1016/j.orggeochem.2018.10.002.

Belt, S. T. (2019), What do IP_{25} and related biomarkers really reveal about sea ice change?, *Quaternary Science Reviews*, *204*, 216-219. doi: 10.1016/j.quascirev.2018.11.025.

Belt, S. T., Smik, L., Brown, T. A., Kim, J. H., Rowland, S. J., Allen, C. S., et al. (2016), Source identification and distribution reveals the potential of the geochemical Antarctic sea ice proxy IPSO25, *Nature Communications*, *7*, 12655. doi: 10.1038/ncomms12655.Belt, S. T., Massé, G., Rowland, S. J., Poulin, M., Michel,

C. & LeBlanc, B. (2007), A novel chemical fossil of palaeo sea ice: IP_{25}, *Organic Geochemistry*, *38*, 16-27. doi: 10.1016/j.orggeochem.2006.09.013.

Belt, S. T. & Müller, J. (2013), The Arctic sea ice biomarker IP_{25}: a review of current understanding, recommendations for future research and applications in palaeo sea ice reconstructions, *Quaternary Science Reviews*, *79*, 9-25. doi: 10.1016/j.quascirev.2012.12.001.

Boon, J. J., Hines, H., Burlingame, A. L., Klok, J., Rijpstra, W. C., Leeuw, J. W. D., et al. (1983), Organic geochemical studies of Solar Lake laminated cyanobacterial mats, *In Advances in Organic Geochemistry 1981 (Edited by Bjoroy M. et al.).* pp. 239 248. Wiley, Chichester.

Bröder, L., Andersson, A., Tesi, T., Semiletov, I. & Gustafsson, Ö. (2019), Quantifying Degradative Loss of Terrigenous Organic Carbon in Surface Sediments Across the Laptev and East Siberian Sea, *Global biogeochemical cycles*, *33*, 85-99. doi: 10.1029/2018GB005967.

Bröder, L., Tesi, T., Andersson, A., Eglinton, T. I., Semiletov, I. P., Dudarev, O. V., et al. (2016), Historical records of organic matter supply and degradation status in the East Siberian Sea, *Organic Geochemistry*, *91*, 16-30. doi: 10.1016/j.orggeochem.2015.10.008.

Brown, T. A., Belt, S. T., Tatarek, A. & Mundy, C. J. (2014), Source identification of the Arctic sea ice proxy IP_{25}, *Nature Communications*, *5*, 4197. doi: 10.1038/ncomms5197.

Brown, T. A., Rad-Menéndez, C., Ray, J. L., Skaar, K. S., Thomas, N., Ruiz-Gonzalez, C., et al. (2020), Influence of nutrient availability on Arctic sea ice diatom HBI lipid synthesis, *Organic Geochemistry*, *141*, 103977. doi: 10.1016/j.orggeochem.2020.103977.

Cai, W.-J., Chen, L., Chen, B., Gao, Z., Lee, S. H., Chen, J., et al. (2010), Decrease in the CO_2 uptake capacity in an ice-free Arctic Ocean basin, *Science*, *329*(5991), 556-559. doi: 10.1126/science.1189338.

Cavalieri, D. J., Gloersen, P., Parkinson, C. L., Comiso, J. C. & Zwally, H. J. (1997), Observed hemispheric asymmetry in global sea ice changes, *Science*, *278*(5340), 1104-1106. doi: 10.1126/science.278.5340.1104.

Coachman, L. K. & Aagaard, K. (1966), On the water exchange through Bering Strait, *Limnology and Oceanography*, *11*, 44-59. doi: 10.4319/lo.1966.11.1.0044.

Collins, L. G., Allen, C. S., Pike, J., Hodgson, D. A., Weckström, K. & Massé, G.

(2013), Evaluating highly branched isoprenoid (HBI) biomarkers as a novel Antarctic sea-ice proxy in deep ocean glacial age sediments, *Quaternary Science Reviews*, *79*, 87-98. doi: 10.1016/j.quascirev.2013.02.004.

Comiso, J. C. (2012), Large decadal decline of the Arctic multiyear ice cover, *Journal of Climate*, *25*(4), 1176-1193. doi: 10.1175/JCLI-D-11-00113.1.

Cronin, T. M., Polyak, L., Reed, D., Kandiano, E. S., Marzen, R. & Council, E. (2013), A 600-ka Arctic sea-ice record from Mendeleev Ridge based on ostracodes, *Quaternary Science Reviews*, *79*, 157-167. doi: 10.1016/j.quascirev.2012.12.010.

de Vernal, A., Radi, T., Zaragosi, S., Van Nieuwenhove, N., Rochon, A., Allan, E., et al. (2020), Distribution of common modern dinoflagellate cyst taxa in surface sediments of the Northern Hemisphere in relation to environmental parameters: The new n= 1968 database, *Marine Micropaleontology*, *159*, 101796. doi: 10.1016/j.marmicro.2019.101796.

Divine, D. V., Korsnes, R. & Makshtas, A. P. (2004), Temporal and spatial variation of shore-fast ice in the Kara Sea, *Continental Shelf Research*, *24*, 1717-1736.

Dukhovskoy, D., Johnson, M. & Proshutinsky, A. (2006), Arctic decadal variability from an idealized atmosphere-ice-ocean model: 1. Model description, calibration, and validation, *Journal of Geophysical Research, 111(C6)*. doi: 10.1029/2004jc002821.

Fahl, K. & Nöthig, E.-M. (2007), Lithogenic and biogenic particle fluxes on the Lomonosov Ridge (central Arctic Ocean) and their relevance for sediment accumulation: Vertical vs. lateral transport, *Deep Sea Research Part I: Oceanographic Research Papers*, *54*(8), 1256-1272. doi: 10.1016/j.dsr.2007.04.014.

Fahl, K. & Stein, R. (2012), Modern seasonal variability and deglacial/Holocene change of central Arctic Ocean sea-ice cover: new insights from biomarker proxy records, *Earth Planetary Science Letters*, *351*, 123-133.

Fernandes, M.-B. & Sicre, M.-A. (2000), The importance of terrestrial organic carbon inputs on Kara Sea shelves as revealed by n-alkanes, OC and $\delta^{13}C$ values, *Organic Geochemistry*, *31*, 363-374. doi: doi.org/10.1016/S0146-6380(00)00006-1.

Gillett, N. P., Kirchmeier-Young, M., Ribes, A., Shiogama, H., Hegerl, G. C., Knutti, R., et al. (2021), Constraining human contributions to observed warming since the pre-industrial period, *Nature Climate Change*, *11*, 207-212. doi: 10.1038/s41558-020-00965-9.

Gordeev, V. V., Martin, J. M., Sidorov, I. S. & Sidorova, M. V. (1996), A reassessment of the Eurasian river input of water, sediment, major elements, and nutrients to the Arctic Ocean, *American Journal of Science*, *296*, 664-691. doi: 10.2475/ajs.296.6.664.

Grebmeier, J. M., Cooper, L. W., Feder, H. M. & Sirenko, B. I. (2006), Ecosystem dynamics of the Pacific-influenced Northern Bering and Chukchi Seas in the Amerasian Arctic, *Progress in Oceanography*, *71*, 331-361. doi: 10.1016/j.pocean.2006.10.001.

Haine, T. W., Curry, B., Gerdes, R., Hansen, E., Karcher, M., Lee, C., et al. (2015), Arctic freshwater export: Status, mechanisms, and prospects, *Global Planetary Change*, *125*, 13-35. doi: 10.1016/j.gloplacha.2014.11.013.

Hill, V., Ardyna, M., Lee, S. H. & Varela, D. E. (2018), Decadal trends in phytoplankton production in the Pacific Arctic Region from 1950 to 2012, *Deep Sea Research Part II: Topical Studies in Oceanography*, *152*, 82-94. doi: 10.1016/j.dsr2.2016.12.015.

Hillaire-Marcel, C. & de Vernal, A. (2008), Stable isotope clue to episodic sea ice formation in the glacial North Atlantic, *Earth Planetary Science Letters*, *268*, 143-150. doi: 10.1016/j.epsl.2008.01.012.

Holmes, R. M., McClelland, J. W., Peterson, B. J., Tank, S. E., Bulygina, E., Eglinton, T. I., et al. (2011), Seasonal and Annual Fluxes of Nutrients and Organic Matter from Large Rivers to the Arctic Ocean and Surrounding Seas, *Estuaries and Coasts*, *35*(2), 369-382. doi: 10.1007/s12237-011-9386-6.

Hörner, T., Stein, R., Fahl, K. & Birgel, D. (2016), Post-glacial variability of sea ice cover, river run-off and biological production in the western Laptev Sea (Arctic Ocean)–A high-resolution biomarker study, *Quaternary Science Reviews*, *143*, 133-149.

Koch, C. W., Cooper, L. W., Grebmeier, J. M., Lalande, C. & Brown, T. A. (2020), Seasonal and latitudinal variations in sea ice algae deposition in the Northern Bering and Chukchi Seas determined by algal biomarkers, *PLoS One*, *15*(4), e0231178. doi: 10.1371/journal.pone.0231178.

Kolling, H. M., Stein, R., Fahl, K., Sadatzki, H., Vernal, A. & Xiao, X. (2020), Biomarker Distributions in (Sub)- Arctic Surface Sediments and Their Potential for Sea Ice Reconstructions, *Geochemistry, Geophysics, Geosystems, 21*(10). doi: 10.1029/2019gc008629.

Köseoğlu, D., Belt, S. T., Smik, L., Yao, H., Panieri, G. & Knies, J. (2018), Complementary biomarker-based methods for characterising Arctic sea ice conditions: A case study comparison between multivariate analysis and the PIP25 index, *Geochimica et Cosmochimica Acta*, *222*, 406-420. doi: 10.1016/j.gca.2017.11.001.

Kraberg, A. C., Druzhkova, E., Heim, B., Loeder, M. J. G. & Wiltshire, K. H. (2013), Phytoplankton community structure in the Lena Delta (Siberia, Russia) in relation to hydrography, *Biogeosciences*, *10*(11), 7263-7277. doi: 10.5194/bg-10-7263-2013.

Lewis, K. M. & Arrigo, K. R. (2020), Ocean Color Algorithms for estimating chlorophyll a, CDOM absorption, and particle backscattering in the Arctic Ocean *Journal of Geophysical Research: Oceans*, *125*(6), e2019JC015706. doi: 10.1029/2019JC015706.

Li, L., Liu, Y., Wang, X., Hu, L., Yang, G., Wang, H., et al. (2020), Early diagenesis and accumulation of redox-sensitive elements in East Siberian Arctic Shelves, *Marine Geology*, *429*, 106309. doi: 10.1016/j.margeo.2020.106309.

Locarnini, R. A., Mishonov, A. V., Antonov, J. I., Boyer, T. P., Garcia, H. E., Baranova, O. K., et al. (2013), World Ocean Atlas 2013, Volume 1: Temperature. S. Levitus, Ed., A. Mishonov Technical Ed., *NOAA Atlas NESDIS 73*, 40 pp.

Massé, G., Rowland, S. J., Sicre, M.-A., Jacob, J., Jansen, E. & Belt, S. T. (2008), Abrupt climate changes for Iceland during the last millennium: evidence from high resolution sea ice reconstructions, *Earth Planetary Science Letters*, *269*, 565-569. doi: 10.1016/j.epsl.2008.03.017.

Moline, M. A., Karnovsky, N. J., Brown, Z., Divoky, G. J., Frazer, T. K., Jacoby, C. A., et al. (2008), High latitude changes in ice dynamics and their impact on polar marine ecosystems, *Annals of New York Academy of Sciences*, *1134*, 267-319. doi: 10.1196/annals.1439.010.

Morison, J., Kwok, R., Peralta-Ferriz, C., Alkire, M., Rigor, I., Andersen, R., et al. (2012), Changing Arctic Ocean freshwater pathways, *Nature*, *481*(7379), 66-70. doi: 10.1038/nature10705.

Morris, K., Li, S. & Jeffries, M. (1999), Meso- and microscale sea-ice motion in the East Siberian Sea as determined from ERS-1 SAR Data, *Journal of Glaciology*, *45*, 370-383.Müller, J., Wagner, A., Fahl, K., Stein, R., Prange, M. & Lohmann, G. (2011), Towards quantitative sea ice reconstructions in the northern North

Atlantic: A combined biomarker and numerical modelling approach, *Earth and Planetary Science Letters*, *306*, 137-148. doi: 10.1016/j.epsl.2011.04.011.

Münchow, A., Weingartner, T. J. & Cooper, L. W. (1999), The summer hydrography and surface circulation of the East Siberian Shelf Sea, *Journal of Physical Oceanography*, *29*(9), 2167-2182. doi: 10.1175/1520-0485(1999)029<2167:TSHASC>2.0.CO;2.

Nair, A., Mohan, R., Crosta, X., Manoj, M. C., Thamban, M. & Marieu, V. (2019), Southern Ocean sea ice and frontal changes during the Late Quaternary and their linkages to Asian summer monsoon, *Quaternary Science Reviews*, *213*, 93-104. doi: 10.1016/j.quascirev.2019.04.007.

Nelson, D. B. & Sachs, J. P. (2014), The influence of salinity on D/H fractionation in dinosterol and brassicasterol from globally distributed saline and hypersaline lakes, *Geochimica et Cosmochimica Acta*, *133*, 325-339. doi: 10.1016/j.gca.2014.03.007.

Nöthig, E. M., Lalande, C., Fahl, K., Metfies, K., Salter, I. & Bauerfeind, E. (2020), Annual cycle of downward particle fluxes on each side of the Gakkel Ridge in the central Arctic Ocean, *Phil. Trans. R. Soc. A*, *378*, 20190368. doi: 10.1098/rsta.2019.0368.

Osadchiev, A., Silvestrova, K. & Myslenkov, S. (2020), Wind-Driven Coastal Upwelling near Large River Deltas in the Laptev and East-Siberian Seas, *Remote Sensing*, *12*(5). doi: 10.3390/rs12050844.

Osadchiev, A. A., Pisareva, M. N., Spivak, E. A., Shchuka, S. A. & Semiletov, I. P. (2020), Freshwater transport between the Kara, Laptev, and East-Siberian seas, *Scientific Reports*, *10*(1), 13041. doi: 10.1038/s41598-020-70096-w.

Overland, J. E. & Wang, M. (2013), When will the summer Arctic be nearly sea ice free?, *Geophysical Research Letters*, *40*(10), 2097-2101. doi: 10.1002/grl.50316, 2013.

Parkinson, C. L., Cavalieri, D. J., Gloersen, P., Zwally, H. J. & Comiso, J. C. (1999), Arctic sea ice extents, areas, and trends, 1978–1996, *Journal of Geophysical Research*, *104*(C9), 20837-20856. doi: 10.1029/1999JC900082.

Park, H., Watanabe, E., Kim, Y., Polyakov, I., Oshima, K., Zhang, X. D., et al. (2020), Increasing riverine heat influx triggers Arctic sea ice decline and oceanic and atmospheric warming, *Science Advances*, *6*(45), eabc4699. doi: 10.1126/sciadv.abc4699.

Peulvé, S., Sicre, M.-A., De Leeuw, J. W., Baas, M. & Saliot, A. (1996), Molecular characterization of suspended and sedimentary organic matter in an Arctic delta, *Limnology and Oceanography*, *4*, 488-497. doi: 10.4319/lo.1996.41.3.0488.

Petrova, V.I., Batova, G.I., Zinchenko, A.G., Kursheva, A.V., Narkevskiy, N.V. (2004), The East Siberian Sea: Distribution, sources, and burial of organic carbon. In: Stein, R. and Macdonald, R.W. (Eds.), *The Organic Carbon Cycle in the Arctic Ocean*, Springer-Verlag, Berlin, pp. 204-212.

Polyakov, I. V., Alekseev, G. V., Bekryaev, R. V., Bhatt, U. S., Colony, R., Johnson, M. A., et al. (2003), Long-term ice variability in Arctic marginal seas, *Journal of Climate*, *16*(12), 2078-2085. doi: 10.1175/1520-0442(2003)0162.0.CO;2.

Ren, J., Chen, J., Bai, Y., Sicre, M.-A., Yao, Z., Lin, L., et al. (2020), Diatom composition and fluxes over the Northwind Ridge, western Arctic Ocean: Impacts of marine surface circulation and sea ice distribution, *Progress in Oceanography*, *186*, 102377. doi: 10.1016/j.pocean.2020.102377.

Rigor, I. G. & Wallace, J. M. (2004), Variations in the age of Arctic sea-ice and summer sea-ice extent, *Geophysical Research Letters*, *31*(9), L09401. doi: 10.1029/2004gl019492.

Salvadó, J. A., Tesi, T., Sundbom, M., Karlsson, E., Kruså, M., Semiletov, I. P., et al. (2016), Contrasting composition of terrigenous organic matter in the dissolved, particulate and sedimentary organic carbon pools on the outer East Siberian Arctic Shelf, *Biogeosciences*, *13*, 6121-6138. doi: 10.5194/bg-13-6121-2016.

Sevastyanov, V. S., Fedulov, V. S., Fedulova, V. Y., Kuznetsova, O. V., Dushenko, N. V., Naimushin, S. G., et al. (2019), Isotopic and Geochemical Study of Organic Matter in Marine Sediments from the Indigirka Delta to the Ice Shelf Border of the East-Siberian Sea, *Geochemistry International*, *57*(5), 489-498. doi: 10.1134/s0016702919050100.

Sevastyanov, V. S., Kuznetsova, O. V., Fedulov, V. S., Fedulova, V. Y., Dushenko, N. V., Naimushin, S. G., et al. (2020), Accumulation of Organic Matter, Heavy Metals, and Rare-Earth Elements in Marine Sediment at Different Distance from the Indigirka River Delta, *Geochemistry International*, *58*(12), 1313-1320. doi: 10.1134/s0016702920120046.

Shindell, D. & Faluvegi, G. (2009), Climate response to regional radiative forcing during the twentieth century, *Nature Geoscience*, *2*(4), 294. doi: 10.1038/ngeo473.

Sicre, M.-A., Ternois, Y., Paterne, M., Martinez, P. & Bertrand, P. (2001), Climatic

changes in the upwelling region off Cap Blanc, NW Africa, over the last 70 kyear: a multi-biomarker approach, *Organic Geochemistry*, *32*(8), 981-990. doi: 10.1016/S0146-6380(01)00061-4.

Smik, L., Cabedo-Sanz, P. & Belt, S. T. (2016a), Semi-quantitative estimates of paleo Arctic sea ice concentration based on source-specific highly branched isoprenoid alkenes: a further development of the PIP25 index, *Organic geochemistry*, *92*, 63-69. doi: 10.1016/j.orggeochem.2015.12.007.

Smik, L., Belt, S. T., Lieser, J. L., Armand, L. K. & Leventer, A. (2016b), Distributions of highly branched isoprenoid alkenes and other algal lipids in surface waters from East Antarctica: Further insights for biomarker-based paleo sea-ice reconstruction, *Organic Geochemistry*, *95*, 71-80. doi: 10.1016/j.orggeochem.2016.02.011.

Sparkes, R. B., Doğrul Selver, A., Gustafsson, Ö., Semiletov, I. P., Haghipour, N. & Wacker, L. (2016), Macromolecular composition of terrestrial and marine organic matter in sediments across the East Siberian Arctic Shelf, *The Cryosphere*, *10*(5), 2485-2500. doi: 10.5194/TC-10-2485-2016.

Speer, L., Nelson, R., Casier, R., Gavrilo, M., Quillfeldt, C. v., Cleary, J., et al. (2017), *Natural Marine World Heritage in the Arctic Ocean, Report of an expert workshop and review process*, Gland, Switzerland: IUCN.112p

Stein, R. & Fahl, K. (2000), Holocene accumulation of organic carbon at the Laptev Sea continental margin (Arctic Ocean): sources, pathways, and sinks, *Geo-Marine Letters*, *20*, 27-36. doi: 10.1007/s003670000028.

Stein, R. & Macdonald, R. W. (2004), *The Organic Carbon Cycle in the Arctic Ocean*, Springer.

Stein, R. & Fahl, K., 2004a. The Laptev Sea: Distribution, Sources, Variability and Burial of Organic Carbon. In: Stein, R. and Macdonald, R.W. (Eds.), *The Organic Carbon Cycle in the Arctic Ocean*, Springer-Verlag, Berlin, pp. 213-237.

Stein, R. & Fahl, K., 2004b. The Kara Sea: Distribution, Sources, Variability and Burial of Organic Carbon. In: Stein, R. and Macdonald, R.W. (Eds.), *The Organic Carbon Cycle in the Arctic Ocean*, Springer-Verlag, Berlin, pp. 237-266.

Stein R. Arctic Ocean Sediments: Processes, Proxies, and Paleoenvironment (2008). *Developments in Marine Geology*, Elsevier, 2: iii. doi.org/10.1016/S1572-5480(08)00014-6.

Stein, R., Fahl, K., Schreck, M., Knorr, G., Niessen, F., Forwick, M., et al. (2016), Evidence for ice-free summers in the late Miocene central Arctic Ocean, *Nature*

Communications, *7*, 11148. doi: 10.1038/ncomms11148.

Stein, R., Fahl, K., Gierz, P., Niessen, F. & Lohmann, G. (2017), Arctic Ocean sea ice cover during the penultimate glacial and the last interglacial, *Nature Communications*, *8*(1), 373. doi: 10.1038/s41467-017-00552-1.

Stocker, T. F., Qin, D., Plattner, G.-K., Tignor, M., Allen, S. K., Boschung, J., et al. (2013), Contribution of working group I to the fifth assessment report of the intergovernmental panel on climate change, *Climate change*.

Stoynova, V., Shanahan, T. M., Hughen, K. A. & de Vernal, A. (2013), Insights into circum-Arctic sea ice variability from molecular geochemistry, *Quaternary Science Reviews*, *79*, 63-73. doi: 10.1016/j.quascirev.2012.10.006.

Tesi, T., Semiletov, I., Hugelius, G., Dudarev, O., Kuhry, P. & Gustafsson, Ö., (2014), Composition and fate of terrigenous organic matter along the Arctic land- ocean continuum in East Siberia: Insights from biomarkers and carbon isotopes., *Geochimica et Cosmochimica Acta*, *133*, 235-256. doi: 10.1016/j.gca.2014.02.045.

Volkman, J. K. (1986), A review of sterol markers for marine and terrigenous organic matter, *Organic Geochemistry*, *9*(2), 83-99. doi: 10.1016/0146-6380(86)90089-6

Vonk, J. E., Sánchez-García, L., Van Dongen, B., Alling, V., Kosmach, D., Charkin, A., et al. (2012), Activation of old carbon by erosion of coastal and subsea permafrost in Arctic Siberia, *Nature*, *489*, 137-140. doi: 10.1038/nature11392.

Wang, Y., Bi, H., Huang, H., Liu, Y., Liu, Y., Liang, X., et al. (2019), Satellite-observed trends in the Arctic sea ice concentration for the period 1979–2016, *Journal of Oceanology and Limnology*, *37*(1), 18-37. doi: CNKI:SUN:HYFW.0.2019-01-002.

Williford, K. H., Ward, P. D., Garrison, G. H. & Buick, R. (2007), An extended organic carbon-isotope record across the Triassic–Jurassic boundary in the Queen Charlotte Islands, British Columbia, Canada, *Palaeogeography, Palaeoclimatology, Palaeoecology*, *244*(1-4), 290-296. doi: 10.1016/j.palaeo.2006.06.032.

Woodgate, R. A., Aagaard, K. & Weingartner, T. J. (2005), Monthly temperature, salinity, and transport variability of the Bering Strait through flow, *Geophysical Research Letters*, *32*, L04601. doi: 10.1029/2004gl021880.

Wu, J., Stein, R., Fahl, K., Syring, N., Nam, S.-I., Hefter, J., et al. (2020), Deglacial to Holocene variability in surface water characteristics and major floods in the

Beaufort Sea, *Communications Earth & Environment*, *1*(27). doi: 10.1038/s43247-020-00028-z.

Xiao, X., Fahl, K. & Stein, R. (2013), Biomarker distributions in surface sediments from the Kara and Laptev seas (Arctic Ocean): indicators for organic-carbon sources and sea-ice coverage, *Quaternary Science Reviews*, *79*, 40-52. doi: 10.1016/j.quascirev.2012.11.028.

Xiao, X., Stein, R. & Fahl, K. (2015a), MIS 3 to MIS 1 temporal and LGM spatial variability in Arctic Ocean sea ice cover: Reconstruction from biomarkers, *Paleoceanography*, *30*(7), 969-983.

Xiao, X., Fahl, K., Müller, J. & Stein, R. (2015b), Sea-ice distribution in the modern Arctic Ocean: Biomarker records from trans-Arctic Ocean surface sediments, *Geochimica et Cosmochimica Acta*, *155*, 16-29. doi: 10.1016/j.gca.2015.01.029.

Yu, Y., Stern, H., Fowler, C., Fetterer, F. & Maslanik, J. (2014), Interannual Variability of Arctic Landfast Ice between 1976 and 2007, *Journal of Climate*, *27*(1), 227-243. doi: 10.1175/jcli-d-13-00178.1.

Zonn, I. S., Kostianoy, A. G. & Semenov, A. V. (2016), Siberian Polynya, Great Siberian Polynya, in *The Eastern Arctic Seas Encyclopedia*, edited, pp. 307-307, Springer International Publishing, Cham.

Zernova, V. V., Nöthig, E. M. & Shevchenko, V. P. (2000), Vertical microalga flux in the northern Laptev Sea (from the data collected by the yearlong sediment trap), *Oceanology*, 40 (6), pp. 801-808.

Zhang, J., Ashjian, C., Campbell, R., Hill, V., Spitz, Y. H. & Steele, M. (2014), The great 2012 Arctic Ocean summer cyclone enhanced biological productivity on the shelves, *Journal of Geophysical Research: Oceans*, *119*(1), 297-312. doi: 10.1002/2013jc009301.

Zhang, Y., Zhang, Y.-Y., Xu, D.-Y., Chen, C.-S., Shen, X.-Y., Hu, S., et al. (2021), Impacts of atmospheric and oceanic factors on monthly and interannual variations of polynya in the East Siberian Sea and Chukchi Sea, *Advances in Climate Change Research*. doi: 10.1016/j.accre.2021.07.005.

Zweng, M. M., Reagan, J. R., Antonov, J. I., Locarnini, R. A., Mishonov, A. V., Boyer, T. P., et al. (2013), World Ocean Atlas 2013, Volume 2: Salinity. S. Levitus, Ed.; A. Mishonov, Technical Ed, *NOAA Atlas NESDIS 74*, 39 pp.

HBIs and sterols in surface sediments across the East Siberian Sea: implications for palaeo sea-ice reconstructions

Liang Su *et al.*

Figure captions

Figure captions 1-6

Figure 1. (a) Map of the western Arctic Ocean showing surface ocean circulation (blue arrows) and sampling locations (black dots and gray dots). The stations in gray feature a strong influence of rivers. The black number represents the serial number of the station (see Table S1 for details). Main study regions: ESS, East Siberian Sea; CS, Chukchi Sea; LS, Laptev Sea (see Figure S1 for details). The dotted and dashed lines in white represent the 20% isolines of September sea-ice concentration for the period 1990-1999 and 2007-2016, respectively. Typical surface circulation: SCC, Siberian coastal current; PWI, Pacific water inflow (ACW-Alaskan Coastal Water; AW-Anadyr Water; BSW-Bering Shelf Water). Rivers are shown in green lines: LR, Lena River; IR, Indigirka River; KR, Kolyma River. (b) The satellite average Summer Sea-Ice concentration (SuSIC) from 1996 to 2015 obtained from NSIDC (https://nsidc.org). The distribution of mean Summer Sea Surface Salinity (SuSSS) and Summer Sea Surface Temperature (SuSST) from 1955 to 2012 are shown in (c) and (d), respectively. The SuSSS and SuSST data were obtained from Locarnini et al. (2013) and Zweng et al. (2013), respectively.

Figure 2. Distribution of (a) TOC, (b) TN and (c) TOC/TN in the surface sediments of ESS and CS. (d) Map showing the average chlorophyll *a* in May-September (1998–2016) in the ESS (GlobColour, https://hermes.acri.fr/). Isolines of September 20% sea-ice concentration for the period 1990-1999 and 2007-2016 are presented in white dotted and dashed lines, respectively (NSIDC, https://nsidc.org).

Figure 3. Concentrations (μg g^{-1} TOC) of phytoplankton biomarkers: (a) brassicasterol and (b) dinosterol; terrigenous biomarkers: (c) campesterol and (d) β-sitosterol in the surface sediments of ESS and CS. Isolines of September 20% sea-ice concentration of for the period 1990-1999 and 2007-2016 are presented in white dotted and dashed lines, respectively (NSIDC, https://nsidc.org).

Figure 4. Concentrations (μg g^{-1} TOC) of HBIs: (a) IP_{25}, (b) HBI-II, (c) HBI-III and (d) HBI-IV in surface sediments. Isolines of September 20% sea-ice concentrations for the period 1990-1999 and 2007-2016 are presented in white dotted and dashed lines, respectively (NSIDC, https://nsidc.org).

Figure 5. Distribution of PIP_{25} and the satellite SuSIC: (a) P_BIP_{25} based on brassicasterol; (b) P_DIP_{25} based on dinosterol; (c) $P_{III}IP_{25}$ based on HBI-III; (d) the satellite average SuSIC from 1996 to 2015 were obtained from NSIDC (https://nsidc.org). September sea-ice concentration of 20% for the period 1990-1999 and 2007-2016 are presented in white dotted and dashed lines, respectively (NSIDC, https://nsidc.org).

Figure 6. Biomarker distribution along 166°E corresponding transect from off the KR estuary to

permanent sea-ice. The upper panel shows the concentrations of HBIs and sterols. The transect of SuSIC is obtained from the satellite average SuSIC from 1996 to 2015 (NSIDC, https://nsidc.org). The lower panel displays the summer salinity of the upper 80 m water depths with isohalines (1955-2012, Zweng et al., 2013). The salinity front between the riverine discharge and open ocean is marked by salinity = 25. The inset map indicates the transect with the SuSSS distribution (more detailed information can be found in Figure 1).

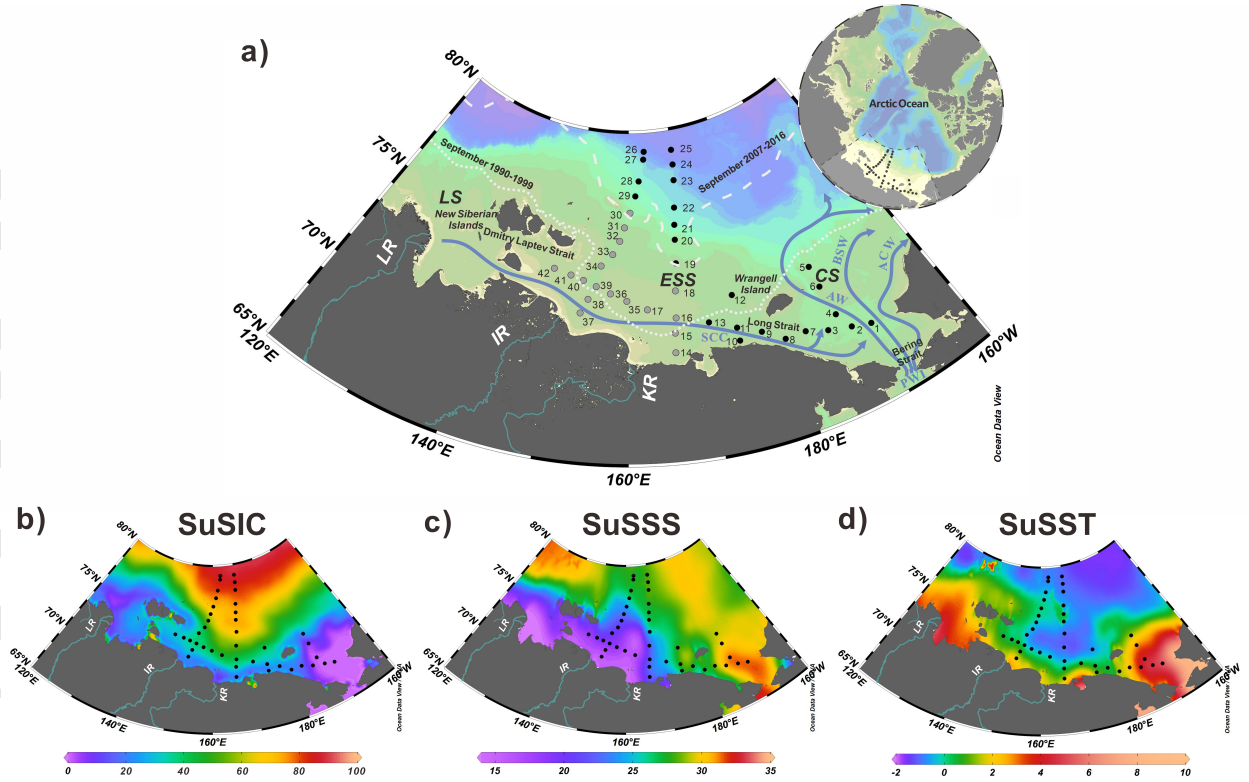

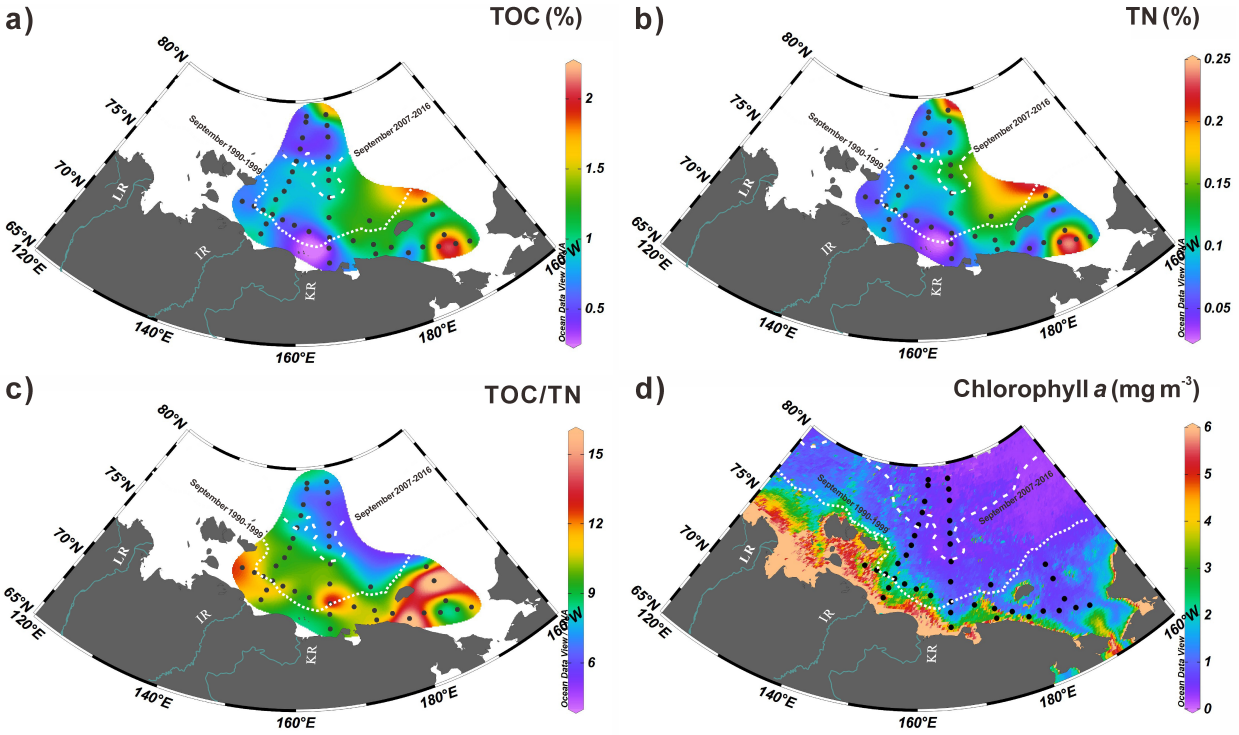

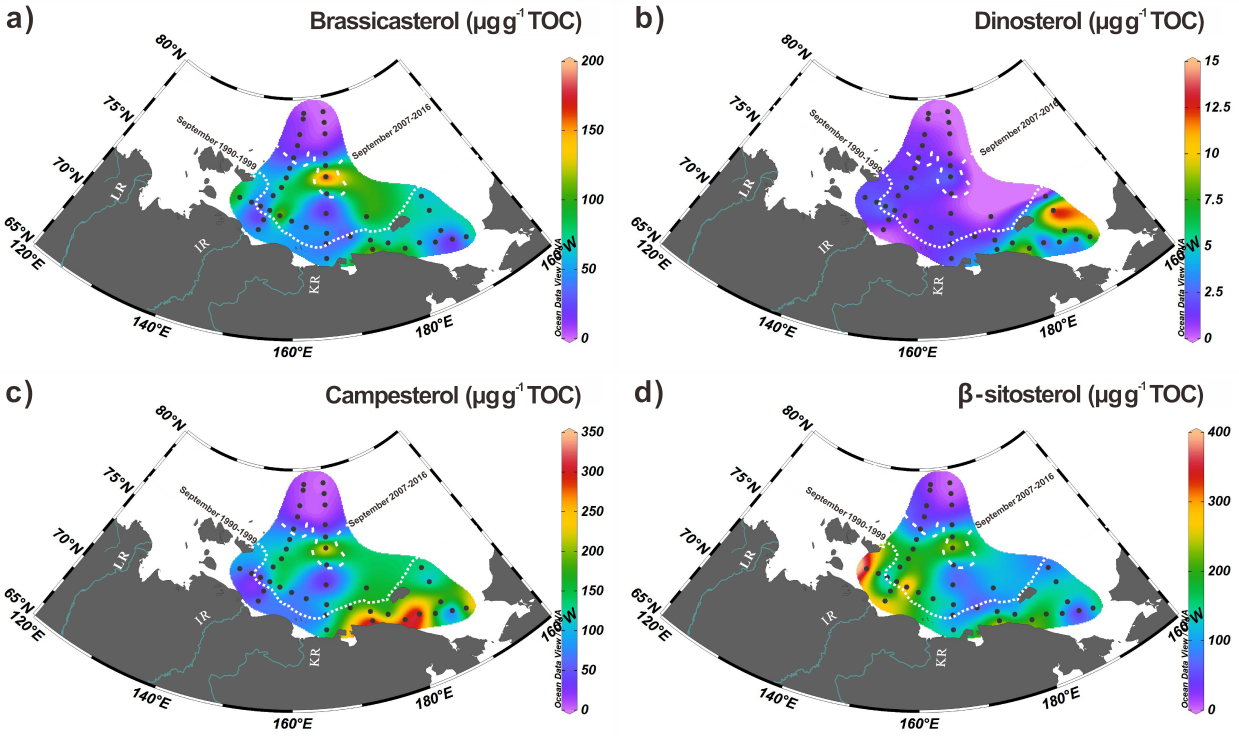

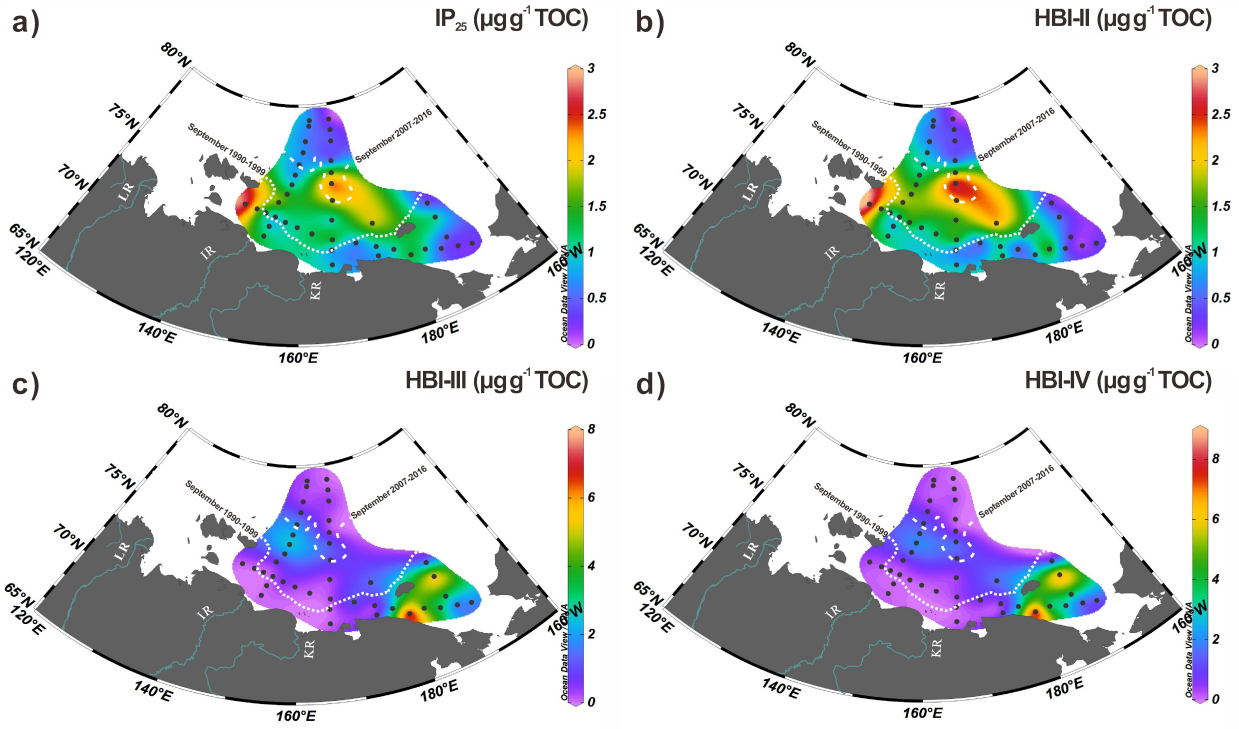

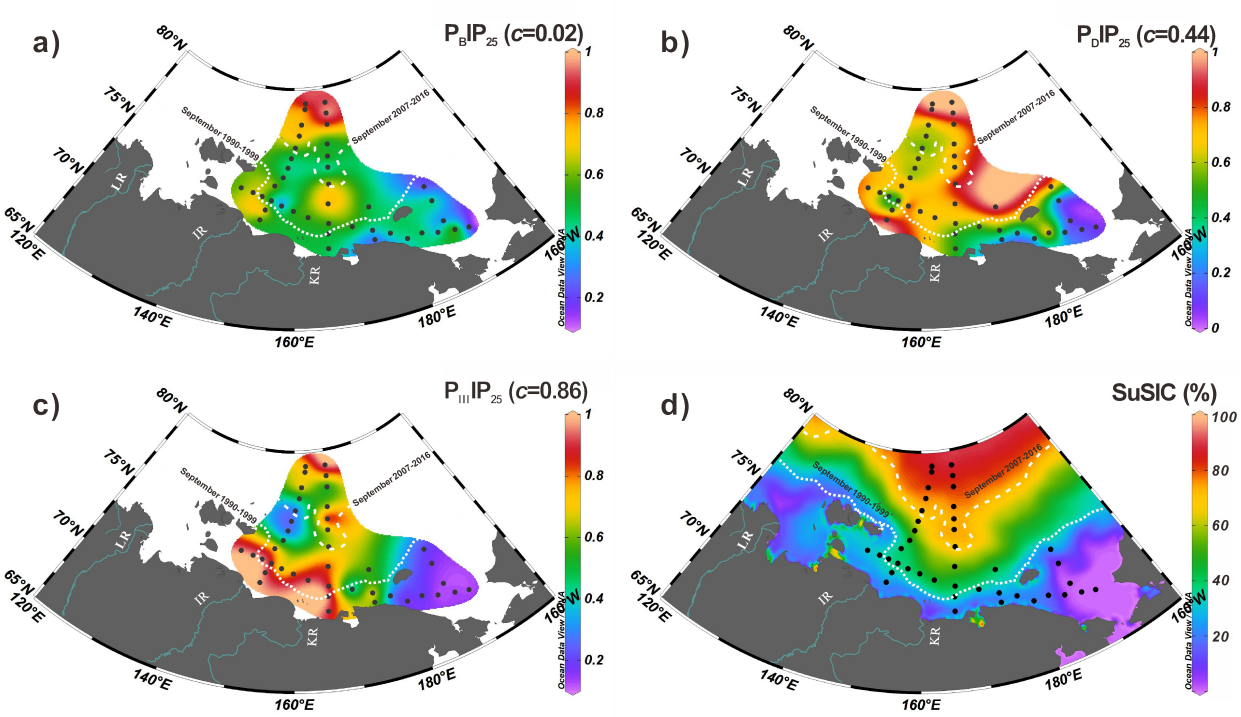

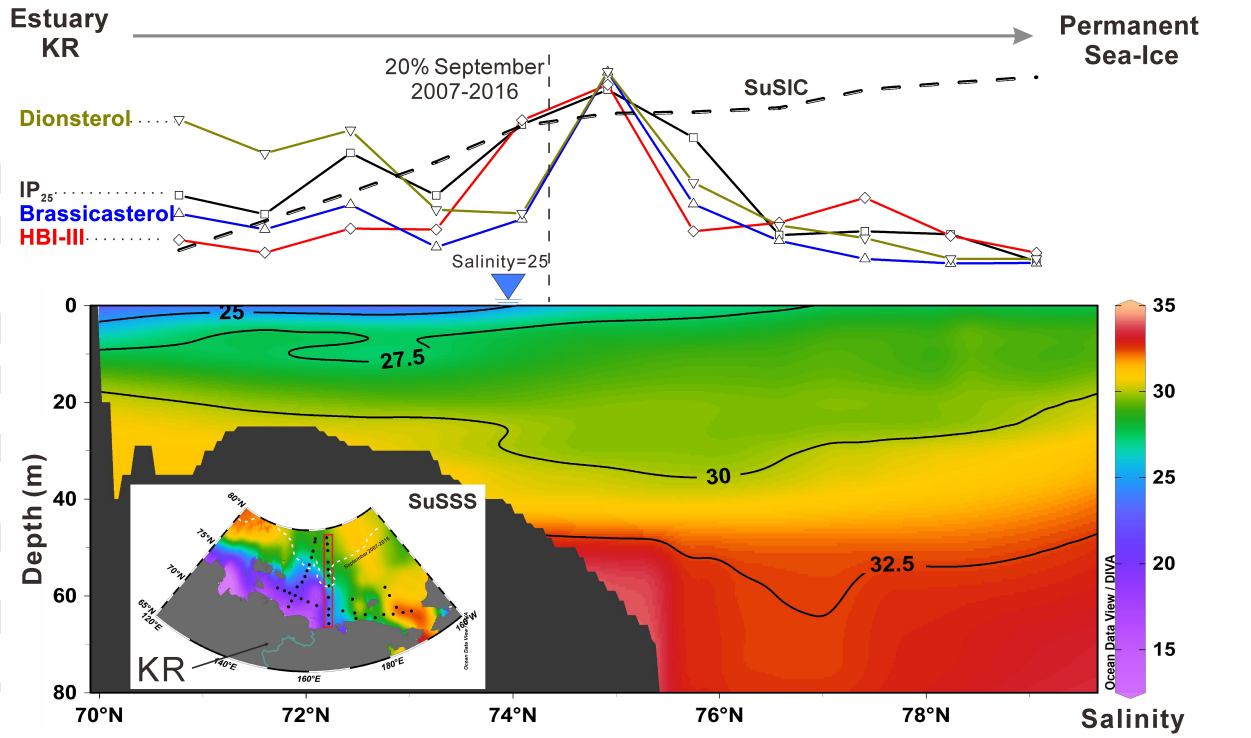

HBIs and sterols in surface sediments across the East Siberian Sea: implications for palaeo sea-ice reconstructions

Liang Su *et al.*

Table 1

Table 1. Comparison of coefficient of determination (r^2) for correlations between PIPs and sea-ice concentrations in summer (SuSIC) and spring (SpSIC).

	Estuarine samples included (n=42)		Estuarine samples excluded (n=24)	
	SpSIC	SuSIC	SpSIC	SuSIC
IP_{25}	0.09	<0.01	0.11	0.01
$P_{III}IP_{25}$ ($c \neq 1$)	0.23	0.12	0.47	**0.73**
$P_{III}IP_{25}$ ($c=1$)	0.22	0.11	0.42	**0.70**
P_BIP_{25}	0.19	0.41	0.27	**0.58**
P_DIP_{25}	**0.51**	**0.46**	**0.65**	**0.66**

All $p<0.01$; Data bold and underlined indicate significant correlation.